

## Preparation and Characterization of Acrylic Polyurethane/Polyaniline Nanocomposite Coatings

Fuyou Lu<sup>1,2,3,4</sup>, Baodong Song<sup>1,\*</sup>, Jixiao Wang<sup>1,2,3,4,\*</sup>

<sup>1</sup> Chemical Engineering Research Center, School of Chemical Engineering and Technology, Tianjin University, Tianjin 300072, PR China

<sup>2</sup> Tianjin Key Laboratory of Membrane Science and Desalination Technology, Tianjin University, Tianjin 300072, PR China

<sup>3</sup> State Key Laboratory of Chemical Engineering, Tianjin University, Tianjin 300072, PR China

<sup>4</sup> Collaborative Innovation Center of Chemical Science and Engineering (Tianjin), Tianjin University, Tianjin 300072, PR China

\*E-mail: [bdson@tju.edu.cn](mailto:bdson@tju.edu.cn), [jxwang@tju.edu.cn](mailto:jxwang@tju.edu.cn)

Received: 8 January 2017 / Accepted: 18 February 2017 / Published: 12 March 2017

---

Acrylic polyurethane and polyaniline (APU/PANI) nanocomposite coatings with excellent protective performance were prepared with physical blending method. Then, the effect of PANI nanowire on the coating's protective and mechanical properties was investigated. The protective performance of APU/PANI nanocomposite coatings was characterized by electrochemical impedance spectroscopy (EIS) technology. After immersion for 58 days in 3.5 wt % NaCl solution at 35 °C, the EIS results interestingly demonstrated that the original coating has the unexpected highest impedance value at about  $1.57 \times 10^{10}$  ohms·cm<sup>2</sup> in all specimens. However, with the increase of PANI nanowire contents, the APU/PANI nanocomposite coating's impedance decreased dramatically and spot corrosion occurred gradually. That is to say, PANI nanowire has the negative effect on the protection performance of the APU nanocomposite coatings system. In addition, the results also indicated that, with increase of PANI nanowire, the APU nanocomposite coating's mechanical behavior deteriorated dramatically and water resistance decreased slightly. These experimental results will provide some helpful insights on study of PANI nanowire modified other coating systems or protective mechanism of PANI.

---

**Keywords:** polyaniline; acrylic polyurethane; coating; EIS; corrosion

### 1. INTRODUCTION

Acrylic polyurethane (APU) coating generally is two components products, the one is isocyanate (as curing agent) and the other is hydroxyl acrylic resin [1, 2]. Ascribed to this coating

structure contains urethane, urea linkages and long carbon chain groups together, APU coating not only has polyurethane coating advantages of good mechanical properties, low temperature curing property and solvent resistance [3, 4], but also has the advantages of acrylic coating, such as light-protection, color-protection and weather resistance [5-7], and is widely applied on furniture surfaces, buildings, automobiles and airplanes [8, 9], etc. But, the corrosion resistance of APU coating is not high enough, and its application in the marine environment is limited. Therefore, it is necessary to modify the APU coating with excellent comprehensive performance.

Polyaniline (PANI), because of its high environmentally-stability [10], easy preparation, low cost, unique chemical property, interesting photoelectric property [11-13], and excellent corrosion resistance property for wide range of metallic substrates (such as, mild steel [14, 15], iron [16, 17], aluminum [18], copper [19] and alloy [20, 21]), has attracted much attention from the science and technology over the past three decades [22]. Recently, researches on organic coatings containing PANI showed that PANI plays the roles of passivation, anode protection and barrier capacity under various conditions [14, 15, 23-25], etc. Of course, our laboratory's previous investigations [26, 27] also showed that PANI added into the epoxy matrix coating can substantially improve the protective performance.

However, the references reveal that the efficiency of PANI on the coatings' protection performance may be controversy. For example, K.A. Thomas et.al [28] reported that the PANI (in polyurethane antifouling coating) caused to the lower impedance in 3.5 wt% NaCl solution. Nevertheless, U.A. Samad et.al [29, 30] found that the PANI improved impedance modulus effectively in epoxy or waterborne epoxy coating. Therefore, it is necessary to do more investigation to make sure whether PANI has an effective anti-corrosion effect in other coating systems. To our best knowledge, there is few report about the exploration of PANI on the APU matrix coating by physical blend method.

Here, APU/PANI nanocomposite coatings were prepared by physical blending method and the effect of PANI nanowire content on the protective performance of APU/PANI nanocomposite coating were monitored by electrochemical impedance spectroscopy (EIS) techniques. In detail, the coatings were applied on a mild-steel substrate and were immersed in 3.5 wt% NaCl solution at 35°C. Simultaneously, the mechanical behaviors of nanocomposite coating was measured by a series of mechanical instruments.

## 2. EXPERIMENTAL SECTION

### 2.1 Materials

Hydroxyl acrylic resin (1107N, Hydroxyl groups content is 3.2 wt%) was obtained from Foshan gaoming tod chemical Ltd. Co., China. HDI biuret (N75, NCO%=16.8 wt%) as curing agent was purchased from Bayer Co., Germany. Organic tin catalyst (DBTDL-T12) was purchased from Shanghai Aladdin Bio-Chem Technology Ltd., China. Butyl acetate (BAC) supplied as thinner was purchased from Tianjin Jiangtian Reagent Ltd. Co., China. PANI nanowire was obtained from

laboratory by rapid chemical oxidation method. All chemical reagents are analytical grade and used without any further purification.

Mild steel plates, 120mm×60mm×3mm (Q235, C: 0.17-0.24%; Si: 0.17%-0.37%; Mn: 0.35-0.65%; P: < 0.03%; S: < 0.03%), were used as substrates for corrosion test. Before the coating applied, the steel plates were grinded with 120#, 600#, 1000# and 1500# emery paper and rinsed with ethanol and acetone, then dried naturally.

## 2.2 Synthesis of PANI nanowires

PANI nanowires were synthesized using a rapid mixing process [31]. In detail, 6.4 mmol aniline was dissolved in 1 mol/L, 40 ml sulfuric acid solution. Similarly, ammonium persulfate (APS) was dissolved in another 1 mol/L, 40 ml sulfuric acid solution. These two prepared solutions cooled down to 0°C. Keeping a stable proportion of aniline and APS is 5:1. Then, rapidly mixing two solutions together and shaking well before polymerization begins. Finally, the mixture was carried out at ice-water bath for 8 hours. The final products were filtrated and washed with ethanol and deionized water until the leachate was colorless. The resulting PANI nanowire was dried at 60 °C for 24 hours in a vacuum.

## 2.3 Preparation of nanocomposite coatings

The hydroxyl acrylic resin, BAC, PANI nanowire and DBTDL-T12 were quantitatively mixed and grinded for 5 times by colloid grinder, getting mixed component A. The N75 diluted by BAC as a component of B. Then, A and B components are mixed according to proposal isocyanate index of 1.2:1. The mixture was homogenized under ultrasonic dispersing condition for 1 min. Finally, it was brushed on the pretreated mild plates uniformly. Specimens were cured at room temperature for 24 hours and then at 60 °C for 12 hours to ensure that the curing process is complete. To avoid pinhole defects of coatings, all the specimens were painted two times identically. The dry thickness of coatings was about 60±10 μm. For the exploration of concentration effects, a series of coatings prepared by adding different contents of PANI nanowire with 0.5%, 1.0%, 1.5%, 2.0% and 2.5%, respectively. An original coating without PANI nanowire was also prepared under the same conditions.

## 2.4 Characterizations

### 2.4.1 Characterization of the morphology

The morphology and size of PANI nanowire was characterized by scanning electron microscopy (SEM) of a JEOL JSM-6700F microscope, transmission electron microscopy (TEM) with JEM-2100F model. The homogeneousness of PANI nanowire in the acrylic resin was observed by a HIROX digital microscope (KH-7700, Japan). The optical photographs of specimens after immersion

for 58 days were recorded by a HD camera. The cross-sectional morphology of coatings after immersion for 58 days was also characterized by SEM.

#### 2.4.2 Anti-corrosion performance of coatings

EIS technique was employed to estimate the protection performance of the nanocomposite coatings. All measurements were conducted on the Princeton STAT Versa electrochemical workstation. A one-compartment cell arrangement with a three electrodes was used for tests. The reference electrode was a saturated calomel electrode (SCE), and the counter electrode (CE) was a graphite electrode. The working electrode (WE) was the coated specimen, and the area of working electrode in contact with 3.5 wt% NaCl solution is approximate  $1.00\text{ cm}^2$ . The measurements were conducted within the frequency range of 0.01 Hz to 100 kHz, using a 10 mV amplitude of alternating voltage. In order to avoid coulombs field effects, all measurements were placed in a Faraday cage.

#### 2.4.3 The wettability of the coatings

Dataphysics OCA15EC contact-angle goniometer is employed to test the coating hydrophilic property by the Sessile Drop Technique. Static contact angles were measured within 1 min by dropping a droplet of water ( $1\ \mu\text{L}$ ) to the coating surface at ambient temperature. All the contact angles measured here were the average of at least three measurements.

#### 2.4.4 Mechanical performance measurements

Mechanical performance of coatings was evaluated in detail just as below: the impact resistance of coatings was tested by QCJ film impact testing machine, The flexibility of coatings was measured by film bending machine (QTY-10A), and the hardness of coatings was tested by pencil hardness tester (QH-Q-A).

## 4. RESULT AND DISCUSSION

The SEM and TEM images of PANI nanowire were presented in Fig. 1(a) and Fig. 1(b), respectively. It is clear that the diameter of the prepared PANI nanowire was about 80~90 nm, and the length was several micrometers. The dispersibility of PANI nanowire in hydroxyl acrylic resin was shown in Fig. 1(c). The optical figure revealed that most of PANI nanowire was dispersed homogeneously in resin. Inevitably, there was also a little slightly aggregation, which was attributed to forming small inextricable knots in the agitating and grinding process. However, these micron aggregation is also effective to improve the protection performance in epoxy coating[32]. The morphology of APU/PANI nanocomposite coating with 2.5% PANI nanowire, was showed in Fig. 1(d). It is obvious that the coating surface was quite smooth and dense, and there was no structural

defects exposing on the upper surface of coatings, which manifested that preparation process of the nanocomposite coatings was successful and guaranteed.

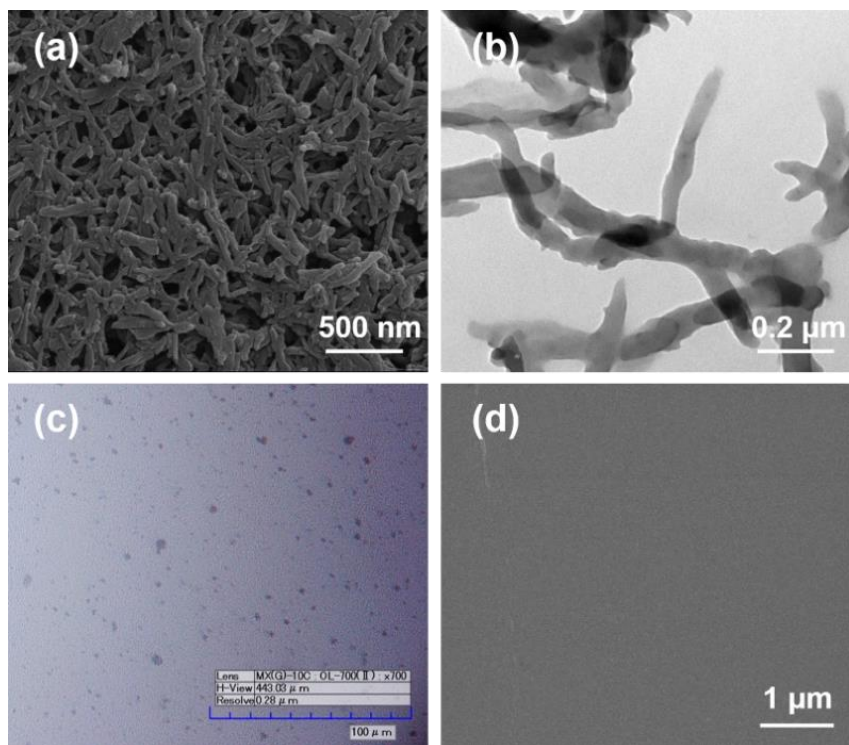


**Figure 1.** (a) SEM image of the PANI nanowire, (b) TEM image of the PANI nanowire, (c) Optical micrograph of hydroxyl acrylic resin blend with PANI nanowire, (d) The morphology of nanocomposite coating with 2.5% PANI nanowire.

Owing to corrosion process of the metals is a mainly electrochemical process, it is appropriate to evaluate the protective performance of organic coatings by electrochemical technique. EIS measurement has become one of the most popular methods to study coatings [33, 34]. In particular, the impedance modulus (expressed as  $|Z|$ ) at low frequency (0.01Hz) can be used to reflect directly anti-corrosion performance of coatings. Bode plots of different samples at different immersion period (in 3.5% wt NaCl solution, at 35 °C) were shown in Fig. 2, respectively. From these curves, it was can be found that the impedance modulus plots changed obviously with the increase of PANI contents in the coatings.

Initially (in the period of immersion for 2 days), both the original coating and coatings filled with PANI nanowire showed very high impedance modulus ( $>10^{11}$  ohms·cm<sup>2</sup>) at 0.01 Hz (Fig. 2a). The Bode curves expressed as a quite straight line with a slope of close to -1. These electrochemical behaviors at initial periods indicates that all the coatings possessed good protective performance [35]. In general, the coating with value of  $|Z|_{0.01\text{Hz}} > 10^8$  ohms·cm<sup>2</sup> is considered as an excellent protection coating. While, the value of  $|Z|_{0.01\text{Hz}} < 10^6$  ohms·cm<sup>2</sup> is considered as a poor protection coating [36-38]. After 10 days immersion in 3.5 wt% NaCl solutions, the Bode plots of the coatings was presented in Fig. 2 b. For the coatings with 2.0 wt% and 2.5 wt% PANI nanowire, the Bode curves are no longer straight lines, along with appearing of a small platform at low frequency, which indicated that these

two coatings had appeared slight corrosion at the interface of coating and metal. While, for original coating and 0.5 wt% PANI coating, there have no corrosion were founded.

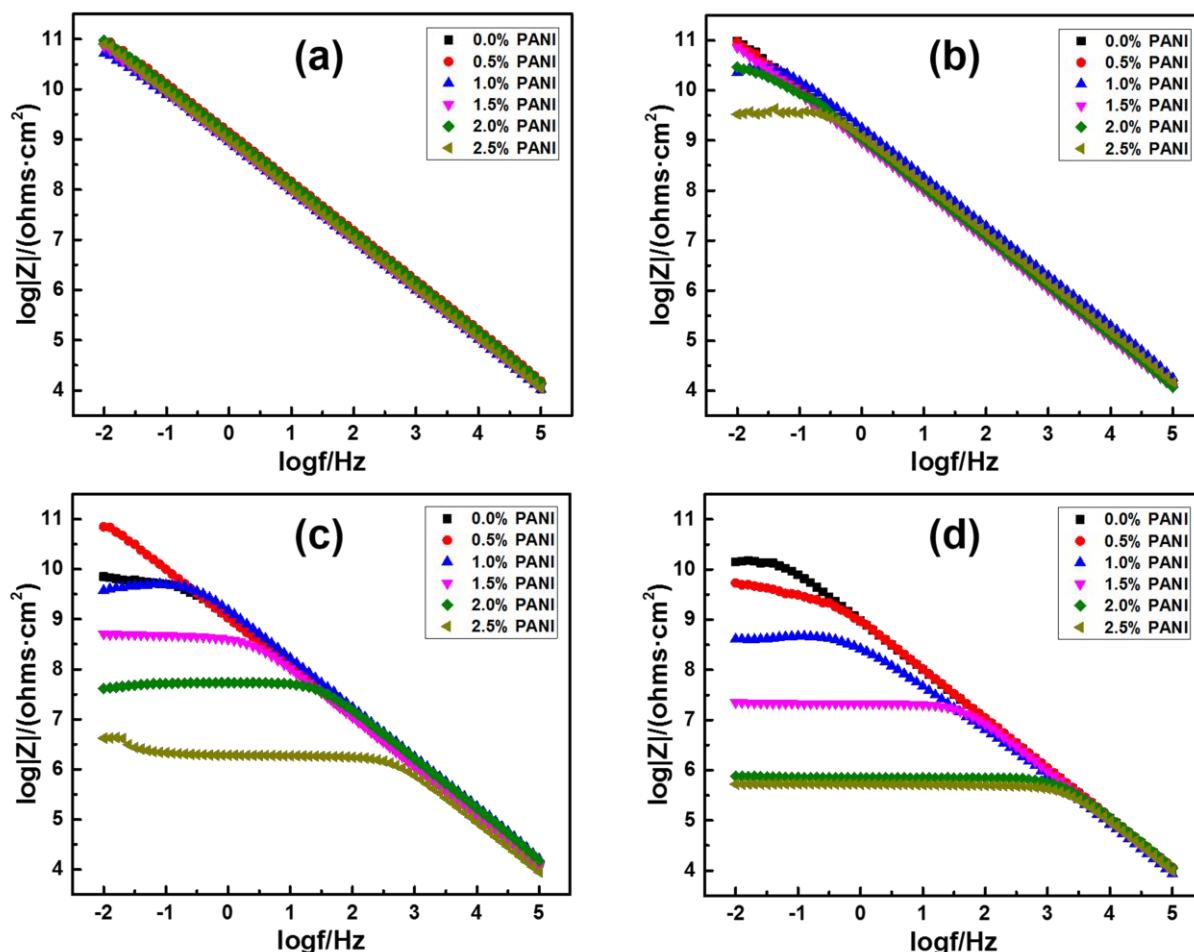


**Figure 2.** Bode plots of coatings in 3.5%, NaCl solution at different immersion time for (a) 2 days, (b) 10 days, (c) 34 days, (d) 58 days ( T 35°C)

Then, immersion test was continued until 34 days, as shown in Fig. 2c, all coatings' impedance modulus were significantly reduced. Finally, when the immersion of samples in 3.5% NaCl solution were lasted for 58 days, the obtained impedance modulus plots were shown in Fig. 2d. Here, for the coatings with the 1.5 wt%, 2.0 wt% and 2.5 wt% PANI nanowire, their impedance modulus at low frequency were already below  $10^8$  ohms·cm<sup>2</sup>, which suggested that the above coatings had lost their effective protection ability to metal substrate. Only the original coating and 0.5% PANI nanowire coating still have excellent protection ability to the substrate (impedance modulus was closed to  $10^{10}$  ohms·cm<sup>2</sup>). It is obvious that the higher the PANI nanowire content in coatings was, the faster impedance modulus of the coatings decreases. These Bode plots tendency was basically consistent with the previous research of PANI modified polyurethane antifouling coatings [28].

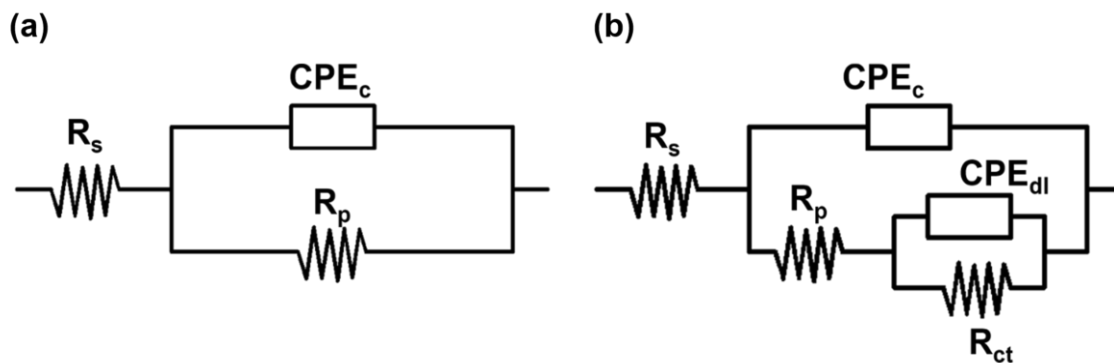


**Figure 3.** Equivalent electrical circuit models selected to analyze the EIS results. (a) Randle’s model (b) Mansfeld model

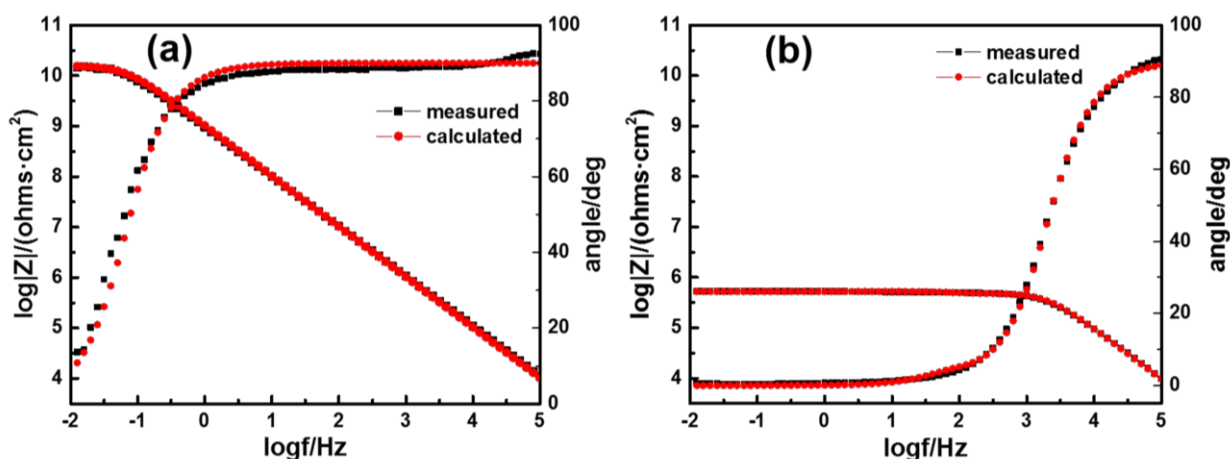


**Figure 4.** Equivalent electrical circuit fitting results of samples after 58 days immersion. (a) 0.0% PANI (b) 2.5% PANI

In order to further illustrate the effect of PANI on the protection ability of APU/PANI coatings, an equivalent electric circuit (EEC) was considered as a model. Typically, the original coating was simulated by Randle’s model [39], as shown in Fig. 3a.

**Table 1.** Fitting values of EEC elements after 58 days immersion

Samples	$R_p/\text{ohms}\cdot\text{cm}^2$	$R_{ct}/\text{ohms}\cdot\text{cm}^2$	$C_c/\text{F}\cdot\text{cm}^{-2}$
0.0% PANI	1.57E10	—	1.54E-10
0.5% PANI	3.91E9	—	1.45E-10
1.0% PANI	2.95E7	4.13E8	1.97E-10
1.5% PANI	8.64E6	1.26E7	1.56E-10
2.0% PANI	7.07E5	6.29E5	1.60E-10
2.5% PANI	4.834E5	4.218E4	1.63E-10

However, the coating with 2.5% PANI nanowire was considered with the Mansfeld model [40], is shown in Fig. 3b. To Mansfeld model, it is thought that the corrosion process had occurred between the coating and metal interface.  $R_s$ ,  $CPE_c$ ,  $R_p$ ,  $CPE_{dl}$ , and  $R_{ct}$  refer to solution resistance, coating capacitance, polarization resistance, double layer capacitance and charge transfer resistance, respectively. Especially for the original and 2.5% PANI coatings, the fitting results for both the impedance modulus and phase angle plots after 58 days immersion were showed in Fig. 4. Accordingly, other coatings were also fitted and the results are presented in Table 1.

For the original coating, the fitting results for the impedance modulus and phase angle plots are shown in Fig.4 (a), and the plots showed good agreement with the experimental results. After 58 immersion, the phase angle still close to  $90^\circ$  in a wide range of frequencies. In combination with Table 1, the  $R_p$  of original coating had a high value at  $1.57 \times 10^{10}$  ohms $\cdot$ cm $^2$ , showing that the coating plays a role of insulating layer, and have excellent barrier effect on the transmission of corrosive medium. However, for the coating with 2.5% PANI nanowire, as shown in Fig.4 (b), on the whole the phase angle was close to  $0^\circ$  in a wide range of frequencies. And the  $R_p$  was  $4.83 \times 10^5$  ohms $\cdot$ cm $^2$ , which implies the electrolyte has reached the interface between coating and metal, and forming a corrosion micro battery. At the same time, the  $R_{ct}$  was only  $4.22 \times 10^4$  ohms $\cdot$ cm $^2$ , demonstrates the corrosion rate was high and occurred corrosion products in great area [41]. In addition, with increase of PANI contents, and the  $C_c$  of coatings increased slightly (under the maximal water absorption conditions, there is no difference of magnitude order.). Due to good electrical conductivity of PANI, PANI accelerated charge transfer once electrochemical corrosion occurs. Thus, as can be seen from Table 1, the  $R_{ct}$  value of coatings reduced obviously with increase of PANI.

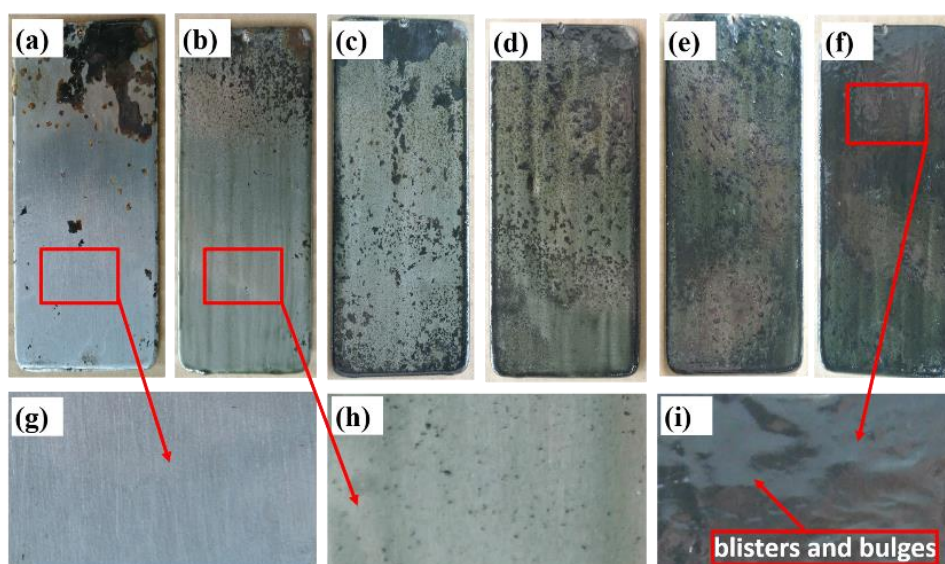


**Figure 5.** Photographs of specimens for 58 days immersion. (a) 0.0% PANI, (b) 0.5% PANI, (c) 1.0% PANI, (d) 1.5% PANI, (e) 2.0% PANI, (f) 2.5% PANI. (g), (h) and (i) was the enlarged region of (a), (b) and (f) respectively

After immersion in 3.5% NaCl solution at 35°C for 58 days, all specimens were dried and keeping them in air for five days. In this process, the samples continue corroding under sufficient air conditions. Finally, the optical photographs were taken and showed in Fig. 5. The figures obviously demonstrate that, there were densely corrosion pits on the coatings which have PANI nanowires. In particular, for the coatings with 1.5 wt% and 2.0 wt% PANI nanowires, a large number of corrosion products were formed. As to coating with 2.5 wt% PANI nanowire, the film had been peeled off from the steel substrate and many blisters and bulges formed. The results demonstrate that PANI decreased the adhesion strength of the coatings during immersion process. Convenient for comparing, the local area of Fig. 5a and Fig. 5b were enlarged and shown as Fig. 5g and Fig. 5h respectively. The enlarged region clearly indicated that the original coating and coating with 0.5 wt% PANI only a few speck of rust appeared. And the original coating was cleaner without corrosion. However, the coating with 0.5% PANI occurred very small corrosion products, but it still had essential ability of protecting metals.

All these electrochemical results reveals the PANI has negative effects on protective performance of APU coatings system. It may be attributed to the reaction occurred between PANI and curing agent from APU coating. Owing to the reaction rate of -NH and -NCO is faster than -OH and -NCO [42], all PANI was cross-linked to the acrylic polyurethane segments by covalent links. Compared with interaction of PANI pigments in epoxy resin matrix coatings, it is thought that these chemical cross-linking of amino group leads to PANI structure lost protective performance and passivation ability.

Water contact angle as a vital characteristic, and is widely used to investigate surface energy and water resistance property. Naturally, the better hydrophobic the coating is, the better protection performance the coating has. Here, the contact angle was used as an auxiliary means to characterize the water resistance property of APU/PANI coatings, and the experimental results are displayed in Fig. 6.

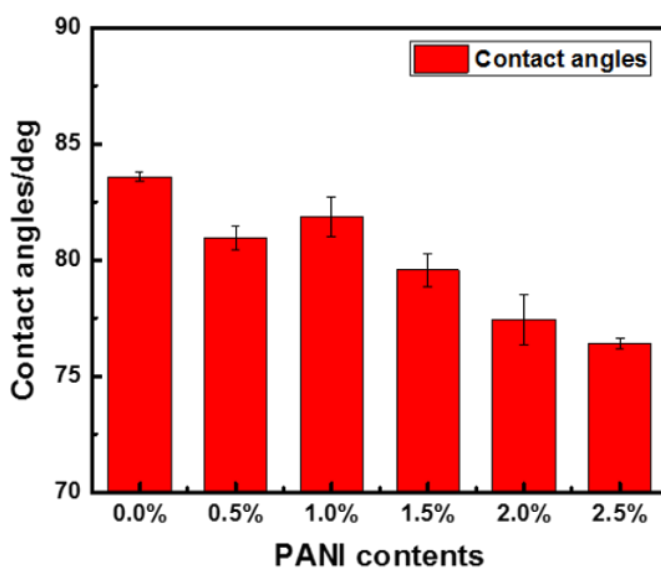


**Figure 6.** Water contact angles of APU/PANI nanocomposite coatings

It can be seen that, the original APU coating had the highest contact angle at  $84^\circ$ , and the coating with 2.5 wt% PANI nanowire possessed lowest contact angle at  $76^\circ$ . On the whole, with the increase of contents of PANI, the contact angle of coatings gradually decreases. This tendency is unfavorable to protection performance of coatings, which was main attributed to good hydrophilicity of PANI [43]. In detail, for one thing PANI enhanced hydrogen bonding forces between the polymer matrix and  $H_2O$  molecule, for another, with the increase of PANI, the coatings surface roughness increased slightly, resulting in the hydrophilicity of coating film becomes better, and aggressive medium penetrating into the APU/PANI nanocomposite coatings easily. Hence, it was coincided that the coatings with PANI occurred corrosion more easily than that of the original APU coating by above EIS analysis.

**Table 2.** Mechanical properties of APU/PANI nanocomposite coatings

PANI context (%)	Pencil hardness	Impact resistance (cm)	Flexibility (mm)
0.0	6H	35	2
0.5	6H	20	3
1.0	6H	20	5
1.5	6H	15	8
2.0	6H	10	12
2.5	6H	10	12

Due to mechanical property of coatings depends on polymer matrixes and additives mainly, consequently, it is studied that the physical and mechanical properties of PANI nanowires on APU coatings system, and test results were presented in Table 2.

The pencil hardness of all the coatings shown as 6H, indicating that the APU coatings have a high hardness. Generally speaking, when the impact resistance values of coatings is greater, and the values of the flexibility is smaller, which results in mechanical properties of the coatings gets better. Nevertheless, the tests results demonstrate that, with the increase of PANI nanowire contents, the impact resistance values decreased, and the flexibility values increased obviously. Namely, the mechanical properties of the coatings became deteriorated dramatically. It is attributed to cross-linking unite of rigid PANI structure, making the molecular polarity and hydrogen-bonding effects increase. Additionally, owing to introduction of reactive activity PANI, enhancing the degree of branched structure of macromolecular chains. Thus, the addition of PANI disrupted intrinsic molecular flexibility and chain mobility of original APU coating.

After immersion for 58 days in 3.5%wt NaCl solution for  $35^\circ\text{C}$ , the coating cross-section were observed and presented in Fig. 7. It is observed that original APU coating had a relatively smooth and homogeneous morphology (from the Fig. 7a). Nevertheless, with the increase of PANI contents, the cross-section images of coatings were becoming increasingly rough and rugged. In particular, for the coating with 1.5%, 2.0% and 2.5% PANI nanowire, the above phenomenon is more obvious. It is considered that, during the coating curing process, the slender APU structure twining around the rigid

PANI structure. Under the conditions of liquid nitrogen cooling, the rapid shrinkage of cross linked crystals, resulting in gaps and cracks occurred between APU-PANI phases regions. Besides, there has been an increasing number of fissures in the cross-section of APU/PANI based coatings, which was attributed to the relaxation of the interphase [44] formed between the APU/PANI components.

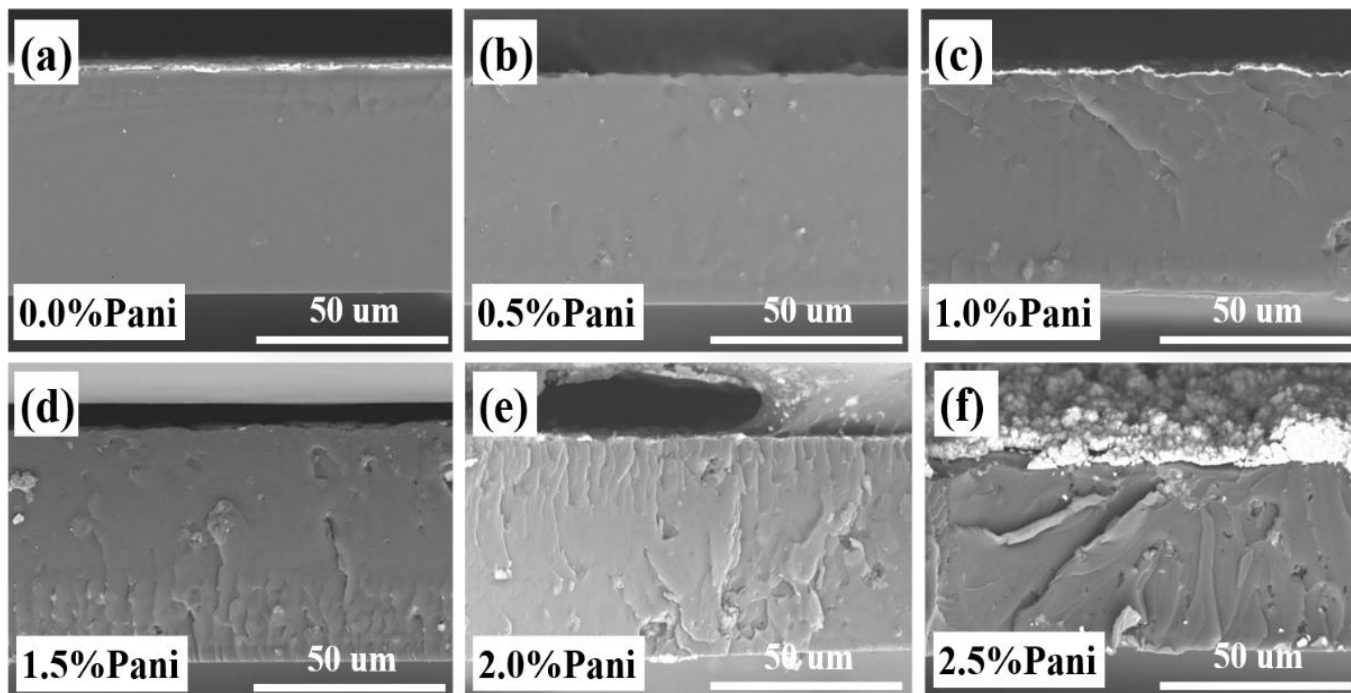


**Figure 7.** Cross sectional SEM images of coatings after 58 days immersion

## 5. CONCLUSIONS

APU/PANI nanocomposite coatings were prepared via the physical blending process. The EIS measurement and visual examination indicate that, the original APU coating manifested excellent corrosion protection performance. Nevertheless, with increase of PANI filled in APU matrix coating, both the protective performance and mechanical properties of APU/PANI nanocomposite coatings become deteriorated dramatically. Rapid reaction occurred between amino group from PANI and the curing agent from APU coating, resulting in PANI structure lost inherent protective performance and passivation ability irreversibly. In addition, the introduction of rigid PANI, making the degree of branching and polarity of the APU/PANI nanocomposite coatings increase, and the coatings mechanical properties became deteriorated greatly. Thus, although PANI is very significant to improve corrosion resistance of the epoxy matrix coatings, it may not the effective component for APU coatings system or other coating systems. The experiment results could provide some helpful insights to further investigate protective mechanism of PANI in organic coatings.

## ACKNOWLEDGEMENTS

This project was supported by National High Technology Research and Development Program (No.2012AA03A611), the Program of Introducing Talents of Discipline to Universities (No. B06006), the Public Science and Technology Research Funds Projects of Ocean (No. 201405013-5), National Natural Science Foundation of China (No.20836006).

## References

1. V. V. Gite, P. P. Mahulikar, D. G. Hundiware, *Prog. Org. Coat.*, 68 (2010) 307.
2. K. D. Weiss, *Prog. Polym. Sci.*, 22 (1997) 203.
3. M. Rashvand, Z. Ranjbar, S. Rastegar, *Prog. Org. Coat.*, 71 (2011) 362.
4. D. Rosu, L. Rosu, C. N. Cascaval, *Polym. Degrad. Stab.*, 94 (2009) 591.
5. K. Hu, W. Kong, X. Fu, C. Zhou, J. Lei, *High Perform. Polym.*, 27 (2015) 930.
6. P. Yan, L. Qiu, *J. Appl. Polym. Sci.*, 114 (2009) 760.
7. H. Erznožnik, T. Razboršek, M. K. Gunde, *Prog. Org. Coat.*, 99 (2016) 47.
8. H. W. Engels, H. G. Pirkl, R. Albers, R. W. Albach, J. Krause, *Angew. Chem. Int. Ed. Engl.*, 52 (2013) 9422.
9. X. Yang, L. Zhu, Y. Chen, B. Bao, J. Xu, *Appl. Surf. Sci.*, 349 (2015) 916.
10. S. Kulandaivalu, Z. Zainal, Y. Sulaiman, *Int. J. Electrochem. Sci.*, 10 (2015) 8926.
11. Y. Zhang, Y. Shao, G. Meng, T. Zhang, P. Li, *J Coat Technol Res.*, 12 (2015) 777.
12. S. de Souza, *Surf. Coat. Technol.*, 201 (2007) 7574.
13. A. F. Baldissera, C. A. Ferreira, *Prog. Org. Coat.*, 75 (2012) 241.
14. A. Mostafaei, F. Nasirpouri, *Prog. Org. Coat.*, 77 (2014) 146.
15. C. Y. Ge, X. G. Yang, B. R. Hou, *J Coat Technol Res.*, 9 (2011) 59.
16. C. Jeyaprabha, S. Sathiyarayanan, G. Venkatachari, *Appl. Surf. Sci.*, 253 (2006) 432.
17. J. Camalet, J. Lacroix, S. Aeiyaich, K. Chane-Ching, P. Lacaze, *Synth. Met.*, 93 (1998) 133.
18. K. G. Conroy, C. B. Breslin, *Electrochim. Acta*, 48 (2003) 721.
19. A. T. Özyılmaz, M. Erbil, B. Yazıcı, *Appl. Surf. Sci.*, 252 (2005) 2092.
20. Y. Shao, H. Huang, T. Zhang, G. Meng, F. Wang, *Corros. Sci.*, 51 (2009) 2906.
21. Y. Zhang, Y. Shao, T. Zhang, G. Meng, F. Wang, *Corros. Sci.*, 53 (2011) 3747.
22. Y. Chen, X. H. Wang, J. Li, J. L. Lu, F. S. Wang, *Corros. Sci.*, 49 (2007) 3052.
23. A. Olad, M. Barati, S. Behboudi, *Prog. Org. Coat.*, 74 (2012) 221.
24. S. Pour-Ali, C. Dehghanian, A. Kosari, *Corros. Sci.*, 85 (2014) 204.
25. T. Siva, K. Kamaraj, S. Sathiyarayanan, *Prog. Org. Coat.*, 77 (2014) 1095.
26. H. Zhang, J. Wang, X. Liu, Z. Wang, S. Wang, *Ind Eng Chem Res.*, 52 (2013) 10172.
27. D. Chu, J. Wang, Y. Han, Q. Ma, Z. Wang, *RSC Advances*, 5 (2015) 11378.
28. K. A. Thomas, S. Nair, R. Rajeswari, A. V. Ramesh kumar, V. Natarajan, *Prog. Org. Coat.*, 89 (2015) 267.
29. U. A. Samad, M. A. Alam, E.-S. M. Sherif, O. Alothman, A. H. Seikh, *Int. J. Electrochem. Sci.*, 10 (2015) 5599.
30. L. Gu, X. Zhao, X. Tong, J. Ma, B. Chen, *Int. J. Electrochem. Sci.*, 11 (2016) 1621.
31. J. Huang, R. B. Kaner, *Angew. Chem. Int. Ed. Engl.*, 43 (2004) 5817.
32. M. R. Bagherzadeh, M. Ghasemi, F. Mahdavi, H. Shariatpanahi, *Prog. Org. Coat.*, 72 (2011) 348.
33. Y. H. Wei, L. X. Zhang, W. Ke, *Corros. Sci.*, 49 (2007) 287.
34. Q.-A. Huang, R. Hui, B. Wang, J. Zhang, *Electrochim. Acta*, 52 (2007) 8144.
35. M. Rashvand, Z. Ranjbar, *Prog. Org. Coat.*, 76 (2013) 1413.
36. D. Ramesh, T. Vasudevan, *Mater. Sci. Appl.*, 03 (2012) 333.
37. M. Bethencourt, F. Botana, M. Cano, R. Osuna, J. Sanchez-Amaya, *WIT Trans. Eng. Sci.*, 48 (2005).

38. M. O'DONOGHUE, R. Garrett, V. DATTA, P. Roberts, T. Aben, *Mater. Performance*, 42 (2003) 36.
39. K. Darowicki, M. Szociński, A. Zieliński, *Electrochim. Acta*, 55 (2010) 3741.
40. M. G. Olivier, M. Poelman, M. Demuynck, J. P. Petitjean, *Prog. Org. Coat.*, 52 (2005) 263.
41. P. Li, T. Tan, J. Lee, *Synth. Met.*, 88 (1997) 237.
42. J. Saunders, R. Slocombe, *Chem. Rev.*, 43 (1948) 203.
43. Z. Fan, Z. Wang, M. Duan, J. Wang, S. Wang, *J Membrane Sci.*, 310 (2008) 402.
44. P. C. Rodrigues, L. Akcelrud, *Polymer*, 44 (2003) 6891.

© 2017 The Authors. Published by ESG ([www.electrochemsci.org](http://www.electrochemsci.org)). This article is an open access article distributed under the terms and conditions of the Creative Commons Attribution license (<http://creativecommons.org/licenses/by/4.0/>).